Simulating Solar Power Plant Variability: A Review of Current Methods

Matthew Lave, Abraham Ellis, Joshua S. Stein

Approved for public release; further dissemination unlimited.

Sandia National Laboratories

Simulating Solar Power Plant Variability: A Review of Current Methods

Matthew Lave
Photovoltaic and Distributed Systems Integration
Sandia National Laboratories
P.O. Box 969, MS-9052
Livermore, CA 94551-0969

Abraham Ellis and Joshua S. Stein
Photovoltaic and Distributed Systems Integration
Sandia National Laboratories
P.O. Box 5800
Albuquerque, New Mexico 87185-1033

Abstract

It is important to be able to accurately simulate the variability of solar PV power plants for grid integration studies. We aim to inform integration studies of the ease of implementation and application-specific accuracy of current PV power plant output simulation methods. This report reviews methods for producing simulated high-resolution (sub-hour or even sub-minute) PV power plant output profiles for variability studies and describes their implementation. Two steps are involved in the simulations: estimation of average irradiance over the footprint of a PV plant and conversion of average irradiance to plant power output. Six models are described for simulating plant-average irradiance based on inputs of ground-measured irradiance, satellite-derived irradiance, or proxy plant measurements. The steps for converting plant-average irradiance to plant power output are detailed to understand the contributions to plant variability. A forthcoming report will quantify the accuracy of each method using application-specific validation metrics.

ACKNOWLEDGMENTS

CONTENTS

FIGURES

TABLES

1. INTRODUCTION

For grid integration studies that examine the effects of adding solar power to the electric grid, it is important to accurately represent the output of solar power plants. However, the accuracy requirements vary depending on the study purpose. Some integration studies focus on balancing area and market operations at the bulk system level (e.g., [1]) and consequently require accurate estimates of plant energy production. Other studies focus on voltage regulation at the distribution level (e.g., [2]) and require accurate representation of the variability (i.e., change with time) of PV system output. For each type of study, a different, timescale dependent metric is needed to measure the accuracy of models for solar PV power plant output.

In this analysis we examine current PV power plant output models to assess the accuracy of simulated PV power plant variability. To our knowledge, these models have not previously been compared to one another and have not been validated for specific grid integration applications, making it difficult to choose the best model for integration studies. We aim to compare methods, data requirements, and ease of implementation for each model, and to test the accuracy of each model by creating application-specific validation metrics.

This work is presented in two parts. This report describes in detail the candidate methods for simulating PV power plant output variability. This allows for both an understanding of the inputs needed to run the models and of the complexity of implementing each model. Section 2 gives an overview of the steps for modeling a PV power plant. Section 3 describes the procedure, implementation, and data requirements of 6 different models for determining plant-average incident irradiance using either ground measurements, satellite measurements, or proxy plant measurements as solar input. The impact that the irradiance to power conversion has on plant output variability is detailed in Section 4, and Section 5 presents the conclusions.

A forthcoming report will develop metrics for quantifying the accuracy of each method and will use these metrics to validate the methods against measured solar power plant data. Validation metrics will focus on three specific impacts that solar variability can have on the electric grid:

a) In the seconds-to-minutes timescale, variability can cause voltage regulation or power quality issues locally on distribution circuits, and can cause additional tap or switching operations on transformers or capacitors.
b) In the minutes-to-hours timescale, variability can increase the amount of regulating and ramping reserves required to balance the system. .
c) In the hours-to-days timescale, variability and uncertainty can increase production cost by reducing the efficiency of generation unit commitment and dispatch.

Combined, the two parts will advise integration studies of the best PV output variability model for their study based on both the ease of implementing the model and the model's performance for their specific application.

2.   PV POWER PLANT MODEL OVERVIEW

Predicting the output of a PV system or PV power plant involves the following modeling steps [3]:

1. Irradiance and Weather
2. Incident Irradiance
3. Soiling, Shading, and Reflection Losses
4. Cell Temperature
5. Module IV Output
6. DC and Mismatch Losses
7. DC to DC Maximum Power Point Tracking
8. DC to AC Conversion
9. AC Losses

Modeling PV output variability requires consideration of all the steps listed above. However, PV power plant output variability arises primarily from variability in the plant-average incident irradiance (steps 1 and 2) variability, and other effects are of second order. Currently, plant-average incident irradiance cannot be directly measured at the spatial and time scales of interest. Instead, plant-average irradiance is modeled based on point sensor irradiance, satellite data, or proxy PV plants. Section 3 of this report describes six simulation models that focus on determining the plant–average irradiance.

PV variability simulations have given less attention to the irradiance to power conversion (steps 3-9). Some studies have attempted to account for irradiance to power losses, such as the use of the System Advisor Model [4] in Hummon, et al. [5] and the use of the Sandia Array Performance Model [6] and Sandia PV Inverter Model [7] in Stein, et al. [8]. Many, though, have simply used a linear multiplier (e.g., [9, 10]) to determine plant power output from plant-average irradiance. We feel that it is important to understand the contributions to variability inherent in irradiance to power conversion, and so Section 4 details the irradiance to power conversion steps and their possible contributions to PV plant power output variability.

3. PLANT-AVERAGE IRRADIANCE SIMULATION METHODS

Methods to simulate the variability in plant-average irradiance vary with respect to both the input data required and the methods used to scale the inputs to account for spatial smoothing. Three types of solar inputs are used: ground point sensor measured irradiance data, satellite-derived irradiance data, and PV plant power output measured at a different location. Table 1 shows the temporal resolution of each solar input and lists the models described in this section. Section 3.4 contains a full comparison of the inputs required by each model.

Table 1: Classification of irradiance averaging models based on input data

Solar Input	Temporal Resolution (time between measurements)	Plant-Average Irradiance Simulation Methods
ground-measured irradiance	<1-sec to ~5-min	• time averaging • low pass filter • Wavelet Variability Model
satellite-derived irradiance	30-min (raw); 1-min (downscaled)	• SolarAnywhere High Resolution • Western Wind and Solar Integration Study II
proxy plant	<1-sec to ~5-min	• plant-to-plant proxy

For plant-average irradiance models, it is important to account for the smoothing within the plant due to the spatial extent of PV modules. Smoothing occurs when a portion of the plant is covered by clouds, but other parts of the plant experience clear-sky or even higher irradiance due to cloud enhancement. As clouds move across the plant, they may uncover part of the PV plant as they cover others. Thus, the variability in the aggregate output for the plant is smoothed compared to the variability at a single point sensor or a single module. This reduction is seen in Figure 1 where the envelope of fluctuations is smaller for a 48MW PV power plant than for a point irradiance sensor. The magnitude of this reduction in variability due to spatial diversity has been observed to change with changing timescale, plant area, and daily meteorological conditions [11].

For each of the models for simulating plant-average irradiance, we describe the general case where both model inputs and outputs represent global horizontal irradiance (GHI). The output of each model is then the plant-average global horizontal irradiance. When applying the models, the plant-average irradiance can be converted to plant-average irradiance incident on plane of the array (POA) (step 2) as needed for tilted or tracking PV arrays using a GHI to POA model (e.g., [12]). Thus, by combining the plant-average irradiance models presented here with a GHI to POA conversion, the plant-average incident irradiance is simulated.
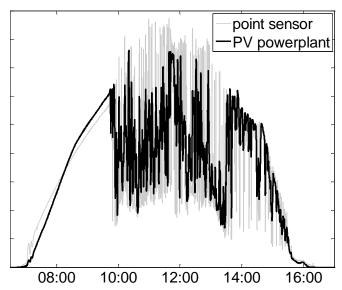
Figure 1: Comparison of the relative variability of a point sensor (light grey) to a 48MW PV power plant (dark black). Y-axis units are scaled to allow for comparison between the point sensor and the power output.

3.1. Methods That Use Ground Measured Irradiance as Input

The simulation methods described in this section start with ground measured irradiance as input. There are a variety of possible ground irradiance measurements that can be used with these methods. Ideally, at least one-year of irradiance measured at 1-second resolution should be used to fully resolve both seasonal effects and short-timescale variability, though shorter periods of representative conditions can be used if that is the only data available. Usually, these methods use only a single irradiance point sensor as input and so in upscaling to plant-average irradiance make the assumption that the irradiance statistics remain homogeneous across the plant footprint. In these cases, it is important to both pick an irradiance sensor in close proximity to the PV plant to be simulated and to ensure that there are not significant meteorological gradients across the simulated plant footprint (e.g., due to sharp terrain changes). When multiple point sensors are available within the plant footprint, they can be averaged to account for statistical inhomogeneity, and then this average can be upscaled to simulated plant-average irradiance.

3.1.1. *Time Averaging*

Description

The simplest method for simulating the spatial smoothing of irradiance over a PV power plant footprint from measured point irradiance data is to apply a temporal smoothing to the irradiance time series, such as the method presented in Longhetto, et al. [13]. Assuming a square-shaped PV plant, the temporal smoothing window, $\bar{t}$, can be estimated as $\bar{t} = \frac{\sqrt{A}}{CS}$, where A is the plant area and CS is the cloud speed. The PV power plant is then simulated by applying a moving average of length $\bar{t}$ to the input point sensor irradiance, where $\bar{t}$ may evolve over time as wind speed changes. Different sizes of PV plants can be simulated by changing the plant area.

Implementation

The time averaging method can be easily implemented in a data processing tool such as MATLAB [14]. Cloud speeds can be obtained from measurements or numerical models [15].

3.1.2. *Low Pass Filter*

Description

Marcos, et al. [9] present a method for simulating PV power plant variability using a low pass filter. Noting the diurnal cycle (periodicity) in solar radiation, the authors applied a Fourier analysis to both point sensor irradiance and measured PV power plant output for plants located in Spain ranging in size from 143 kWp to 9.5MWp. Signals were normalized by $G^* = 1000 \text{ W m}^{-2}$ for irradiance inputs and the plant rated capacity P^* for power inputs to allow for direct comparison between irradiance and power. The point sensor Fourier spectra were found to have a linear region matching a function of the form $f^{-0.7}$, where f is the frequency. In contrast, the Fourier spectra of the power plants had two distinct linear regions, one matching the same function form $f^{-0.7}$ at low frequencies (long timescales), and another at high frequencies matching a function of the form $f^{-1.7}$, meaning that short-timescale fluctuations decay much more rapidly for the power plants versus the point sensor, as seen in Figure 2. The cross point where these two linear regions meet is termed the cut-off frequency, f_c.
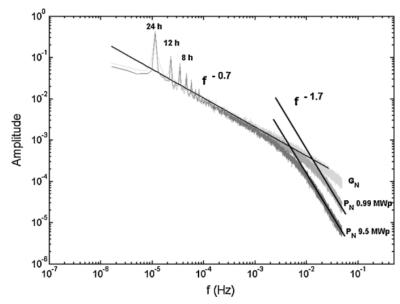

Figure 2: (Fig. 4 in Marcos, et al. [9]) Spectrum of the irradiance G_N recorded at Milagro, outpower P_N at Sesma (0.99MW; 0.8MW) and Milagro (9.5MW; 7.243MW) during 1 year. The linear region for the larger frequencies of the power spectrums can be well fit by a function of the form $f^{-1.7}$.

By comparing the various sized PV plants, intuition was confirmed that the bigger the PV plant, the higher the cut-off frequency. The best-fit curve of cut-off frequencies over all of the plants was $f_c = 0.0204 \times A^{-0.4997}$. By rounding slightly, we see that the cutoff frequency scales with the square root of the area, $f_c = \frac{0.02}{\sqrt{A}}$. Based on this, the transfer function

$$\frac{P(t)}{G(t)} = \frac{K}{\frac{\sqrt{S}}{2\pi * 0.02}s + 1}$$

was proposed, where $G(t)$ is the GHI time series, $P(t)$ is the simulated power output time series, $K = \frac{G^*}{P^*}$, and S is the plant area in hectares.

Implementation

To apply the transfer function to a time series of discrete GHI measurements, we must convert the transfer function from an analog to a digital filter. To do this, we can use a bilinear transformation to map the transfer function from the s-plane (analog) into the z-plane (digital). The formal definition for the transformation is $z = e^{\frac{s}{f}}$, where f is the sampling frequency of the measured time series, but for the bilinear transformation, this is approximated as $s = 2f\frac{z-1}{z+1}$. Through this substitution, the transfer function can be written as

$$\frac{P(z)}{G(z)} = \frac{K(z+1)}{B(z-1)+(z+1)},$$

where $B = \frac{2f\sqrt{S}}{2\pi * 0.02}$ is defined for clarity. By dividing by z and $(1 + B)$, we achieve the transfer function in the typical form used for digital filters:

$$\frac{P(z)}{G(z)} = \frac{\frac{K}{1+B}+\frac{K}{1+B}z^{-1}}{1+\left(\frac{1-B}{1+B}\right)z^{-1}}.$$

One way to use this digital filter function is the MATLAB function "filter." The inputs needed by "filter" are the measured GHI time series and the coefficients of the digital filter, which are found from the typical form of the digital filter: $a(1) = 1$, $a(2) = \frac{1-B}{1+B}$, $b(1) = \frac{K}{1+B}$, and $b(2) = \frac{K}{1+B}$. The output will then be the smoothed irradiance signal, representing plant-averaged irradiance.

3.1.3. *Wavelet Variability Model*

Description

The wavelet variability model (WVM) [10] is a way to simulate PV power plant output by using the top hat wavelet transform to apply different amounts of spatial smoothing at different timescales. The first step of the WVM is to convert the measured irradiance into a clear-sky index by dividing by the expected clear-sky irradiance. This results in a time series that has value 1 during clear-sky conditions, and values less than 1 when clouds are obstructing the sun. A wavelet transform is then used to decompose the clear-sky index into wavelet modes $w_{t^*}(t)$ at various timescales, t^*, which represent cloud-induced fluctuations at each timescale.

To determine how much smoothing to apply to each wavelet mode, the correlations between pairs of PV modules within the plant are estimated using the equation

$$\rho\left(d_{m,n}, t^*\right) = \exp(-\frac{d_{m,n}}{\frac{1}{2}CS\,t^*}),$$

where $d_{m,n}$ is the distance between modules m and n. The distance between modules is estimated based on input specifications about the plant: the plant footprint (area covered) and the density of PV modules within the plant. Correlations are simulated for all N pairs of modules in the PV plant, and then aggregated to find the variability reduction VR at each timescale:

$$\text{VR}(t^*) = \frac{N^2}{\sum_{m=1}^{N}\sum_{n=1}^{N}\rho(d_{m,n}, t^*)}.$$

Each wavelet mode of the irradiance clear-sky index $w_{t^*}(t)$ is divided by the square root of the corresponding $\text{VR}(t^*)$ to create simulated wavelet modes of the entire power plant, $w_{t^*}^P(t)$. Figure 3 shows an example wavelet decomposition of the irradiance clear-sky index and the simulated plant averaged wavelet modes. By applying an inverse wavelet transform to these scaled wavelet modes, the clear-sky index of area-averaged irradiance over the whole power plant is obtained. Finally, this is converted into plant averaged irradiance by multiplying by the clear-sky expected irradiance.

Implementation

Implementation of the WVM involves more steps than the two previously discussed methods. First, a clear-sky model (e.g., Ineichen and Perez [16]) should be used to create the clear-sky index. Next, the top hat wavelet transform of the clear-sky index should be obtained. The top hat wavelet is not native to, for example, MATLAB's wavelet toolbox, but is relatively simple to code as the differences of moving averages with different temporal windows. For example, the 4-second wavelet mode is the 4-second moving average minus the 8-second moving average.

Based on the plant footprint and density, discrete points can be used to simulate PV modules within the plant to compute the distances between modules. Cloud speeds obtained from measurements or models, as mentioned above, are combined with distances to determine correlations at each timescale. From these correlations, it is straightforward to compute the variability reduction VR and apply the scaling at each wavelet mode. The inverse wavelet transform for the top hat wavelet is simply the summation of wavelet modes.
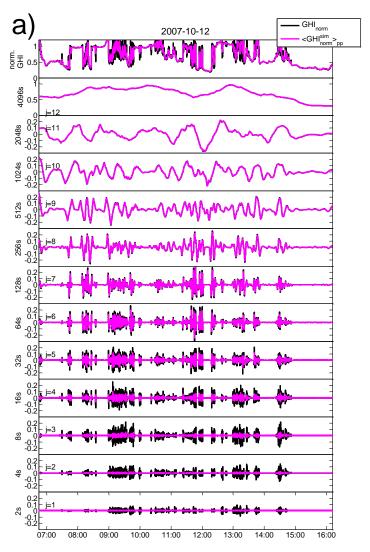
Figure 3: (Fig. 5a in Lave, et al. [10]) Top most plots show clear-sky index time series; and bottom 12 plots show wavelet modes for Ota City on October 12, 2007. Black lines are based on the clear-sky index of the measured GHI while the magenta lines show the simulated spatial average clear-sky index accounting for spatial smoothing across the PV plant.

3.2. Satellite Measured Irradiance as Input

The models described in the previous section all require one or more ground irradiance sensors in close proximity to the PV plant to be simulated. In some cases, however, no measurements exist, or the period of record is not long enough to ensure representative results. Because of this, some methods use satellite-based irradiance as input. Satellite imagery covers most of North America through the GOES satellites at up to 0.01° by 0.01° resolution (approximately 1 by 1 km at 23° latitude), with images captured once every 30-minutes. Both methods discussed in this section use irradiance derived from GOES imagery, though additional satellites exist that cover other areas in varying levels of detail, and similar methods can be applied to other areas. The extensive coverage area and typically long period of record (>10 years) for satellite-based irradiance make these data attractive for PV plant modeling.

16

3.2.1. *Clean Power Research: SolarAnywhere*

Description

The Clean Power Research SolarAnywhere High Resolution [17] product delivers irradiance at 1-minute time intervals over a 0.01° by 0.01° grid covering most of North America. Satellite measurements at 30-minute intervals are used as inputs to a model that downscales to simulated 1-minute time series. The downscaling is achieved by advecting clouds between the two satellite images with a timestep of 1-minute. At each minute, the irradiance is determined based on the image created by the simulated cloud advection. The SolarAnywhere High-Resolution simulated irradiance has been shown to match the variability of ground-measured irradiance reasonably well, as shown in Figure 4. It is worth noting that the size of the grid cells (~1km^2) used in this dataset contain approximately the same area as a 30MW utility-scale PV plant. This, combined with the averaging inherent in advecting the clouds from one image to the next, may lead to an underestimation of the variability at short timescales for smaller PV plants.
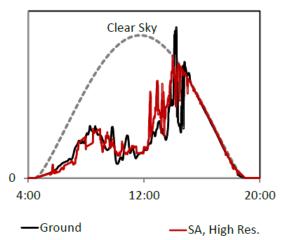
Figure 4: (Fig. on slide 13 in Hoff [17]) Comparison of ground measurements to the SolarAnywhere High Resolution data.

Implementation

The SolarAnywhere High Resolution methods have not been rigorously documented in a public work, and so it would be difficult to exactly follow the same methods. Additionally, the excessive amounts of data (0.01° by 0.01°at 1-minute resolution for 1-year or longer time record) required to be processed would likely be very difficult for an individual user to manage. The satellite to irradiance model is fairly well documented (e.g., Perez, et al. [18]), and 0.1° by 0.1, 1-hour Solar Anywhere data for 1998 through 2009 is available through the National Solar Radiation Database [19], but this is likely not sufficient temporal or spatial resolution for variability studies. Thus, in order to work with the SolarAnywhere High Resolution data, one would have to purchase the data from Clean Power Research.

3.2.2. *Western Wind and Solar Integration Study Dataset II*

Description

For use in the Western Wind and Solar Integration Study (WWSIS), Hummon, et al. [5] used a combination of downscaling and upscaling to simulate 1-minute, plant-average irradiance data for 2007. To achieve the downscaling, ground-measured irradiance was collected at 7 sites at 1-minute temporal resolution. From the clear-sky index of these ground measurements, 5 different classifications of the sky conditions were obtained, ranging from consistently clear or cloudy to partially variable to sharply variable. By combining the ground measurements with satellite measurements, a probabilistic lookup table was created, showing the probability of having any of the sky conditions given a satellite image with certain distance-weighted statistical values for the "patch" of satellite data covering ~4500 km^2 surrounding a ground site. Using patches allowed for better definition of the sky conditions than using a single grid cell.

In order to simulate the 1-minute irradiance at a given site, 1-hour satellite-derived irradiance patches were used as inputs. Based on the probabilistic lookup tables, a sky condition state was assigned for each hour, and the clear-sky index was simulated at 1-minute resolution based on the variability statistics of that sky condition state. The exact method used to synthesize a downscaled irradiance time series varied by sky condition. For a full description, of the downscaling, see Hummon, et al. [5]. The upscaling of the irradiance data to represent plant average irradiance was performed following the Marcos, et al. [9] method described in Section 3.1.2. The WWSIS dataset was found to agree reasonably with measured data at most sites [20].

It is worth noting a similar study by Stein, et al. [8], which also used hourly satellite data as input, but varied in the downscaling and upscaling methods. The hourly satellite irradiance was downscaled by creating a library of more than 5,000 one-day sequences of ground measured irradiance at 1-minute resolution. The library day which had hourly-averages that best matched the hourly satellite data at each study site was used to represent 1-minute irradiance at the study site. Special care was given not to duplicate library days to maintain proper correlations between sites. Since the library days were based on point sensor measurements, they were upscaled to simulate plant-average irradiance using the Longhetto, et al. [13] time-averaging method.

Implementation

The method could be followed after a rigorous reading and duplication of Hummon, et al. [5]. However, for most applications, if 2007 is an appropriate year for the study and the study locations are in the southwest U.S., it would probably be best to request the data from the National Renewable Energy Laboratory.
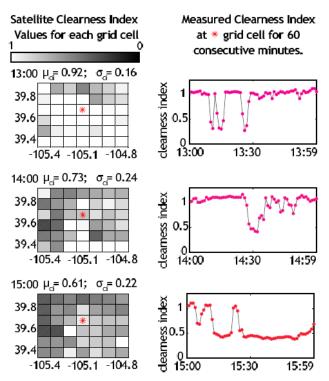
Figure 5: (Fig. 3 in Hummon, et al. [5]) Three consecutive hours (from 1 pm to 3 pm) on Aug. 10, 2005 at SRRL. The spatial pattern shows a trend towards increasing cloudiness over the afternoon..

3.3. Proxy Plant

Description

Power measurements from a monitored, existing power plant can be used as a proxy for simulating a proposed PV plant. For example, the variability of a monitored 20MW plant could be used as a proxy for a hypothetical 20MW PV plant to be built near the current plant. Plants smaller than the monitored plant can be simulated by selecting a smaller subset of the monitored plant (e.g., 10MWs of a 20MW plant), but it is difficult to accurately simulate larger PV plants since this method does not directly account for spatial smoothing. Additional corrections for the available solar resource, module temperature, and module orientation must be made to ensure a reasonable simulation. Consideration should be given to whether the cloud patterns at the monitored plant are similar enough to the simulated plant. In many cases, even small spatial separations can cause significant meteorological differences, resulting in large error in the proxy method useless.

Implementation

Implementation will depend on data availability. If, for example, measurements were known for a PV plant in Las Vegas, NV, those could be used as a proxy for simulating a similar-sized PV plant a short distance away, such as one in Henderson, NV. If the Henderson plant to simulate were smaller, then a sample of the inverters at the Las Vegas plant could be used instead of the whole plant. Large errors would likely result if using a Las Vegas plant as a proxy for a Seattle,

19

WA plant due to the significant meteorological differences between the two locations, so care should be taken to match meteorological conditions when using the proxy method. As a first step, topographical features should be matched (i.e., use a coastal city as a proxy for another coastal city), and more detailed comparisons of the irradiance variability should be performed when possible.

3.4. Input Requirements and Availability

In choosing a method to simulate the plant-average irradiance, it is important to understand the input requirements. Table 2 is a quick reference of the inputs needed for each method. In some cases, the simulation method may be dictated by the available data.

Table 2: Comparison of inputs for the 6 plant-average irradiance simulation methods.

Solar Input	Simulation Method	Inputs Required
ground-measured irradiance	time averaging	point sensor irradiance; cloud speed; plant area
	low pass filter	point sensor irradiance; plant rated capacity; plant area
	Wavelet Variability Model	point sensor irradiance; plant footprint, density of PV coverage, cloud speed
satellite-derived irradiance	SolarAnywhere High Resolution	time series of satellite images (to follow procedure) or money (to purchase SolarAnywhere product)
	Western Wind and Solar Integration Study II	satellite-derived irradiance at multiple locations; ground measured irradiance at 1-min temporal resolution (to create lookup table); plant rated capacity; plant area
proxy plant	plant-to-plant proxy	power output from nearby plant; plant rated capacity

The three methods based on ground-measured irradiance have similar input requirements, except that the low pass filter method does not require cloud-speed as an input. Cloud speed can be reasonably estimated from radiosonde measurements or from numerical weather forecasts [15]. The plant properties (footprint/area, rated capacity, and density of PV) should all be specified by the integration study or easily approximated (e.g., by assuming a square-shaped plant). Therefore, only the availability of point sensor irradiance data will dictate whether the ground-measured irradiance based methods can be used. Measured point sensor irradiance time series are common, and are often publicly available (e.g., the NREL Measurement and Instrumentation Data Center [11]). For variability studies, real-time data is not required, and historical data may increase the number of available irradiance time series. Many irradiance sensors have been installed for many years, and so have a long period of record allowing for capture of seasonal

and annual trends. Since the time resolution of the simulated power output is the same as the input point sensor irradiance, high-frequency (e.g., 1-second) irradiance time series are needed to simulate short-timescale effects. The exact temporal resolution of point sensor irradiance needed will depend on the study purpose.

The SolarAnywhere High Resolution method may be more limited. It requires a time series of visible satellite images at native satellite resolution (0.01° by 0.01°). While theoretically these are available publically (e.g., from NOAA [9]), the data storage and processing requirements mean integration studies would likely not attempt this method and instead would purchase the processed SolarAnywhere High Resolution product. Data availability would then be determined by the study budget and the coverage area of SolarAnywhere.

The WWSIS method requires both satellite-derived irradiance values over a large area surrounding the PV plant to be simulated, and ground irradiance measurements at 1-minute temporal resolution to create the lookup table of sub-hourly irradiance statistics. The 0.1° by 0.1° resolution satellite data required is available through the National Solar Radiation Database (NSRDB) [19], and ground irradiance measurements are relatively easy to find, as mentioned above. Thus, input data should be available over the NSRDB coverage area (and other areas with sufficient satellite coverage) if an integration study chose to use the WWSIS method to simulate irradiance.

The proxy-plant method requires power output measurements from a nearby PV power plant. These are difficult to obtain as this information is usually considered proprietary by plant owners and operators. Additionally, since most PV power plants are newly built, the period or record for power measurements is short, making it difficult to accurately capture seasonal or annual trends. Just as for the ground irradiance methods, high-frequency measurements are needed to capture short-timescale effects, further limiting data availability as some plants are only monitored at low frequency (e.g., 15-minutes).

4.   IRRADIANCE TO POWER MODELS AND VARIABILITY EFFECTS

To be useful to grid integration studies, the plant-average irradiance simulated using the methods listed in section 3 must be converted to plant power output. In this section we describe the steps to convert from incident irradiance to AC power output, with a focus on the contributions to PV plant variability. We also mention models that can be used to simulate each step.

4.1. Step 3: Soiling, Shading, and Ground Reflection

Factors such as shading, soiling, or unusual ground reflections can lead to more or less irradiance reaching the plant's PV modules. Module soiling typically increases slowly over long timescales, but can change almost instantaneously when precipitation or maintenance cleans the modules. Shading and reflection losses may vary rapidly. For example, row-to-row shading can be instantaneous and lead to a significant drop in plant output. Ground-reflected irradiance can be significantly increased by snow covering the ground and then be reversed by melting.

The effects of soiling, shading, and ground reflection are typically small, and in most cases, a constant multiplier (e.g., in PVWatts [21]) can be used to reasonably model these effects. However, it is important to remember that isolated events (e.g., rain cleaning a module, the onset of one panel shading another, or snow melting) may lead to a significant contribution to plant variability that is not capture by a linear model. More detailed models do exist if plant properties (e.g., module layout) are known. For example, 3-D shadow modeling (e.g., [22]) can be used to predict shading effects. Kimber, et al. [23] propose a model of soiling-related PV system performance degradation based on a detailed study of soiling of systems in California.

4.2. Step 4: Cell Temperature

As cell temperatures increases, PV modules become less efficient at converting incident irradiance into DC power. The decrease in efficiency depends on the PV technology being used, but a rule of thumb is that silicon modules' DC power output is reduced by 0.5% per °C of cell temperature increase.

Cell temperatures are the biggest contributor to non-linearity when converting plant-average irradiance to plant power. Cell temperatures scale the PV plant output: cool cells will have a higher maximum output than warm cells under the same irradiance conditions. Because of this, plants often produce maximum power output in the late spring when temperatures are cool instead of in the summer when maximum irradiance is incident on the plant but temperatures are high. This scaling affects PV plant variability in that the magnitude of variability is partially dependent on the cell temperatures within the plant. Additionally, quick changes in cell temperatures (e.g., due to increased wind cooling) can contribute to plant variability.

However, cell temperatures are rarely measured and instead must be approximated using a model, typically involving ambient temperature, wind speed, and irradiance. For example, in the Sandia Photovoltaic Array Performance Model [6], the module temperature T_m is modeled as $T_m = E\{e^{a+b\,WS}\} + T_a$, where E is the incident solar irradiance (W m^{-2}), WS is the wind speed at 10m height, T_a is the ambient air temperature, and a and b are empirically determined

coefficients based on the type of PV module. Most cell temperature models are steady-state, i.e., they assume that PV cell temperature responds instantaneously to changes in air temperature or irradiance. In contrast, many PV modules have sufficient thermal mass that cell temperatures change over a time scale of several minutes. A more advanced transient temperature model [24] has been evaluated by Luketa-Hanlin and Stein [25], and seems to better follow temperature fluctuations at short time scales, which is important for variability analysis.

4.3. Steps 5-6: Module I-V Output and DC Mismatch Losses

Beyond incident irradiance and temperature, there can be further losses on the DC side which contribute to the variability of the PV power plant. Each module can be represented by its own I-V curve and an associated maximum power point (MPP). The I-V curve changes as the irradiance and temperature change. When modules are connected in series to construct a string and connected to an inverter with a maximum power point tracker, the current flowing through each module must be the same, and therefore, because of slight differences in the MMP of the modules there will be some amount of DC mismatch. Because the output of each module is changing dynamically as irradiance and temperature change, the combined MPP will vary and contribute to power output variability in a way that is not linear with respect to irradiance.

In our judgment, these losses are relatively small (e.g., based on MacAlpine, et al. [26]) because by design, modules in the same string will be electrically similar, and will be proximal and hence will see similar irradiance and temperature conditions. Thus, the effect on the variability in overall plant output of DC side losses is also likely to be minimal. However, there are a variety of models for simulating the I-V curves or points on the I-V curves of PV modules. Single diode models for simulating the whole I-V curve include PVSyst [18] and the De Soto "Five-Parameter" Model [27]. Point models, which usually predict the maximum power point or other important points on the I-V curve (V_{OC}, V_{SC}, etc.) include the Sandia Photovoltaic Array Performance Model [6] and PVWatts [21]. Both single diode and point models assume a homogeneous plant with the same irradiance and cell temperature at every module and so anisotropy in the plant may lead to errors in these models.

4.4. Steps 7-9: DC to AC Losses

DC to AC conversion efficiency depends on the inverter specifications, and can change as a function of AC output power, DC voltage, and, where applicable, inverter output power factor. Typical grid-tied inverter efficiencies exceed 95% in most operating conditions. However, inverter operation can impact PV plant variability. Inverters are limited in AC output by their nominal rated capacity. When an inverter achieves its maximum AC output, called inverter saturation or clipping, it will have a cutoff effect that will scale the PV plant AC power output. For example, a 500kW AC inverter will be limited to this output level, even if the input DC power exceeds this rating. Increases in DC power production (positive ramps) will have no effect on plant AC power output variability when the inverter is saturated. Inverter saturation is especially important to consider as many PV power plants are intentionally designed with more DC capacity than inverter AC rating and so may often saturate.

Inverters can also introduce short-timescale fluctuations. Inverters track the changing MPP of the combined I-V curves of PV arrays, and different inverters have different tracking algorithms.

Some inverters have time lags in finding the MPP, and while searching or when abruptly changing power points may contribute to plant variability. Inverter models include the Sandia Inverter Model [7] and the Driesse Inverter Model [28]. Both require inverter-specific performance parameters.

Further losses can occur in the AC transmission of power due to AC wiring losses or transformer losses. In most cases, there will not be significant variability in these losses, and a constant multiplier (e.g., 0.99 as in PVWatts [21]) will be appropriate.

5.   CONCLUSION

This report aims to inform grid integration studies regarding available methods to simulate PV power plant output for their specific study. We have described six different methods which use either ground measurements, satellite measurements, or proxy plant measurements as input. The way to implement each method was described to provide an understanding of its ease of use. Additionally, the input data requirements and availability were compared between the models. In some cases, the information presented in this report will be sufficient to determine which method or subset of methods will be feasible to use. For example, if no local ground irradiance or power measurements were available, a study might be forced to use one of the satellite data methods.

In most cases, though, more than one method may be feasible and hence model accuracy should also be considered. In a follow-on analysis we will evaluate the methods described in this report by defining application-specific validation metrics to test each method's performance at simulating power plant variability at timescales relevant to the three main areas of concern: voltage flicker (seconds to minutes), grid regulation (minutes to hours), and load balancing (hours to days). Using these validation metrics, each simulation method will be compared to measured PV plant output, and the method's accuracy will be quantified for each application. Together, this report and the follow-on analysis will allow integration studies to choose the best PV output simulation method for their study based the ease of implementing the method, the method's input data requirements, and the method's accuracy for the study's application.

REFERENCES

[1]   D. Lew and R. Piwko, "Western wind and solar integration study," National Renewable Energy Laboratory, Tech. Report NREL/SR-550-47434, 2010.

[2]   R. Broderick, J. Quiroz, M. Reno, A. Ellis, J. Smith, and R. Dugan, "Time Series Power Flow Analysis for Distribution Connected PV Generation," Sandia National Laboratories SAND2013-0537, 2013.

[3]   J. Stein, "The Photovoltaic Performance Modeling Collaborative (PVPMC)," presented at the IEE Photovoltaic Specialists Conference Austin, TX, 2012.

[4]   System Advisor Model (SAM). https://sam.nrel.gov.

[5]   M. Hummon, E. Ibanez, G. Brinkman, and D. Lew, "Sub-Hour Solar Data for Power Systems Modeling from Static Spatial Variability Analysis," presented at the 2nd International Workshop on Integration of Solar Power in Power Systems, Lisbon, Portugal, 2012.

[6]   D. King, W. Boyson, and J. Kratochvil, "Photovoltaic Array Performance Model," SAND2004-3535, 2004.

[7]   D. King, S. Gonzalez, G. Galbraith, and W. Boyson, "Performance Model for Grid-Connected Photovoltaic Inverters," Sandia National Laboratories SAND2007-5036, 2007.

[8]   J. Stein, C. Hansen, A. Ellis, and V. Chadliev, "Estimating Annual Synchronized 1-Min Power Output Profiles from Utility-Scale PV Plants at 10 Locations in Nevada for a Solar Grid Integration Study," presented at the 26th European Photovoltaic Solar Energy Conference and Exhibition, Hamburg, Germany, 2011.

[9]   J. Marcos, L. Marroyo, E. Lorenzo, D. Alvira, and E. Izco, "From irradiance to output power fluctuations: the PV plant as a low pass filter," *Progress in Photovoltaics: Research and Applications,* vol. 19, pp. 505-510, 2011.

[10]   M. Lave, J. Kleissl, and J. S. Stein, "A Wavelet-Based Variability Model (WVM) for Solar PV Power Plants," *Sustainable Energy, IEEE Transactions on,* vol. PP, pp. 1-9, 2012.

[11]   M. Lave, J. Stein, and A. Ellis, "Analyzing and Simulating the Reduction in PV Powerplant Variaiblity Due to Geographic Smoothing in Ota City, Japan and Alamosa, CO," presented at the IEEE Photovoltaic Specialists Conference, Austin, TX, 2012.

[12]   R. Perez, P. Ineichen, R. Seals, J. Michalsky, and R. Stewart, "Modeling daylight availability and irradiance components from direct and global irradiance," *Solar Energy,* vol. 44, pp. 271-289, 1990.

[13]   A. Longhetto, G. Elisei, and C. Giraud, "Effect of correlations in time and spatial extent on performance of very large solar conversion systems," *Solar Energy,* vol. 43, pp. 77-84, 1989.

[14]   MATLAB 2013a. Natick, Massachusetts: The MathWorks, Inc. , 2013.

[15]   M. Lave and J. Kleissl, "Cloud speed impact on solar variability scaling – Application to the wavelet variability model," *Solar Energy,* vol. 91, pp. 11-21, 2013.

[16]   P. Ineichen and R. Perez, "A new airmass independent formulation for the Linke turbidity coefficient," *Solar Energy,* vol. 73, pp. 151-157, 2002.

[17]   T. Hoff, "Integrating PV into Utility Planning and Operation Tools," presented at the CPUC-DOE High Penetration Solar Forum, La Jolla, CA, 2013.

[18]   R. Perez, P. Ineichen, K. Moore, M. Kmiecik, C. Chain, R. George*, et al.*, "A new operational model for satellite-derived irradiances: description and validation," *Solar Energy,* vol. 73, pp. 307-317, 2002.

[19]   S. Wilcox. (2012). *National Solar Radiation Database 1991-2010 Update*. http://rredc.nrel.gov/solar/old_data/nsrdb/1991-2010/

[20]   C. Hansen, "Validation of Simulated Irradaince and Power for the Western Wind and Solar Integration Study, Phase II," Sandia National Laboratories SAND2012-8417, 2012.

[21]   T. Hoff and R. Perez, "Predicting Short-Term Variaiblity of High-Penetration PV," presented at the American Solar Energy Society, Denver, CO, 2012.

[22]   PV*SOL Expert. Valentin Software, http://www.valentin.de/en/products/photovoltaics/12/pvsol-expert.

[23]   A. Kimber, L. Mitchell, S. Nogradi, and H. Wenger, "The Effect of Soiling on Large Grid-Connected Photovoltaic Systems in California and the Southwest Region of the United States," in *Photovoltaic Energy Conversion, Conference Record of the 2006 IEEE 4th World Conference on*, 2006, pp. 2391-2395.

[24]   A. D. Jones and C. P. Underwood, "A thermal model for photovoltaic systems," *Solar Energy,* vol. 70, pp. 349-359, 2001.

[25]   A. Luketa-Hanlin and J. Stein, "Improvement and Validation of a Transient Model to Predict Photovoltaic Moduel Temperature," Sandia National Laboratories SAND2012-4307, 2012.

[26]   S. MacAlpine, M. Brandemuehl, and R. Erickson, "Quantifying Mismatch Losses in Small Arrays," presented at the 2013 Sandia PV Performance Modeling Workshop, Santa Clar, CA, 2013.

[27]   W. De Soto, S. A. Klein, and W. A. Beckman, "Improvement and validation of a model for photovoltaic array performance," *Solar Energy,* vol. 80, pp. 78-88, 2006.

[28]   A. Driesse, P. Jain, and S. Harrison, "Beyond the curves: Modeling the electrical efficiency of photovoltaic inverters," in *Photovoltaic Specialists Conference, 2008. PVSC '08. 33rd IEEE*, 2008, pp. 1-6.

DISTRIBUTION

1	MS1033	Abraham Ellis	6112
1	MS1033	Joshua Stein	6112
1	MS1033	Robert Broderick	6112
1	MS1033	Clifford Hansen	6112
1	MS9052	Matthew Lave	6112
1	MS0899	Technical Library	9536 (electronic copy)